



Full State Pose Estimation Using a Satellite Imager

by

D.P. Theron

*Dissertation presented for the degree of Masters of
(Electronic Engineering) in the Faculty of Engineering at
Stellenbosch University*

Supervisor: Prof. H.W. Jordaan
Dr. S. Busch

2025



To God, my Wife and my Mother

ACKNOWLEDGEMENTS

- * Prof. H.W. Jordaan, thank you for all your patience and guidance through this journey.
- * Pinkmatter for your financial support for taking the risk of investing in me and my future. I will be eternally grateful. Thank you for letting me feel like part of the company and taking such good care of me during the visits.
- * Clarissa, my wife, thank you for all your love and support during the difficult times.
- * My Mother, words cannot describe how much you meant to me during my masters degree.
- * My friend and colleagues in the ESL, especially Brandon Chetty, Dane Groves and Mark Msonko, who put up with my 'new productivity hacks' and 'crazy ideas', but also keeping me on track.
- * God, for all your guidance, support, love and faith in me, even though I didn't deserve it.

“ *Whether you think you can or you can't, you're right.* ”

– Mr. Henry Ford

DECLARATION

By submitting this dissertation electronically, I declare that the entirety of the work contained therein is my own, original work, that I am the sole author thereof (save to the extent explicitly otherwise stated), that reproduction and publication thereof by Stellenbosch University will not infringe any third party rights and that I have not previously in its entirety or in part submitted it for obtaining any qualification.

Date: 1 September 2025
.....

Copyright © 2025 Stellenbosch University
All rights reserved.

ABSTRACT

Pose estimation on nanosatellites is still an on going topic of interest. It is important for satellite to know there position and attitude to do accurate target tracking. Traditional solutions to the pose estimation problem is mainly star trackers, which looks at the constalations of stars to determine the attitude and GPS to determine the position of the satellite along with other sensors like magnetometers and coarse sun sensors.

In this thesis, a sensor is developed that utilises the onboard satellite imager, to estimate the position and the attitude of the satellite. The sensor uses a camera model to take pictures of the Earth surface, a feature detector is ran on the image using scale invariant feature transform (SIFT) to identify and establish corospondance of features. A full state kinematic estimator using the extended Kalman Filter (EKF) based on the simultaneous localisation and mapping (SLAM) approach. The filter makes used of feature vectors and feature discriptors detected on the image. This is used to estimate attitude and position of the satellite.

An simulation environment in MATLAB is developed to propagate a satellite and determine the ground truth pose. Several traditional sensors like the star tracker and magnetometer and GPS to be able to compare the Earth Tracker and create the possiblity to fuse the sensors and determine the accuracy. Results show that the filter estimates the system states successfully. It is concluded that ...

UITTREKSEL

TABLE OF CONTENTS

LIST OF FIGURES

LIST OF TABLES

NOMENCLATURE

VARIABLES AND FUNCTIONS

CONSTANTS

ω_e Rotation speed of the Earth

c A constant.

FUNCTIONS

f A function.

VARIABLES

x A variable.

ACRONYMS AND ABBREVIATIONS

DEFINITIONS

VARIABLES AND FUNCTIONS

CONSTANTS

ω_e Rotation speed of the Earth

c A constant.

FUNCTIONS

f A function.

VARIABLES

x A variable.

INTRODUCTION

1.1 PROBLEM BACKGROUND

- Satellites are getting smaller - Because this leads to satellites having reduced costs and timelines - This is enabled by the miniaturisation of electronics
 - One of the big industries in satellites is remote sensing - Remote Sensing is the application where satellites are used to monitor the Earth - One of the applications is to take images of the Earth
 - This leads to the problem that high accuracy is needed to take images of the targets on the Earth's surface - COTS components which is mainly used on small satellites lack the accuracy needed - Magnetometers is too low of an accuracy - Star Trackers have the right accuracy, but is expensive

1.2 PROPOSED SOLUTION

- Proposed solution is to develop an estimation algorithm that can estimate the full state of the satellite - The Full State of a Satellite is its position in Space and its attitude or its orientation in space. - The satellite uses the imager itself to determine position and attitude. - This can lead to reduce costs as the satellite is using an instrument which is already onboard the satellite. - Utilising the components when it is idle - Observing the target directly

1.3 DOCUMENT OUTLINE

- Chapter 2: Will investigate previous sensors that is being used to determine Pose - Previous techniques estimating the pose - Some light touching on feature detection as this is crucial to the pose estimation system

- Chapter 3: Will introduce the modelling of the system - Rigid Body Kinematics - Position Kinematics - Attitude Kinematics - Kalman Filters - Extended Kalman Filters
- Chapter 4: Measurement Generation - Feature detection - PinHole Camera Model. - The Plant - The Plant Model - The Measurement Model
- Chapter 5: State estimation - The Extended Kalman Filter - Update Step - Prediction Step - Simulator
- Chapter 6 is results
- Chapter 7 is Conclusion - Future Work

CHAPTER 2

LITERATURE

2.1 INTRODUCTION

2.2 SATELLITE POSITION AND ATTITUDE DETERMINATION SYSTEMS

2.2.1 POSITION DETERMINATION METHODS

2.2.2 ATTITUDE DETERMINATION SYSTEMS

2.3 EARTH OBSERVATION SATELLITE SYSTEMS AND IMAGING TECHNOLOGIES

2.3.1 HERITAGE EARTH OBSERVATION MISSIONS

2.3.2 COMMERCIAL EARTH OBSERVATION SATELLITES

2.3.3 CAMERA TECHNOLOGIES IN EARTH OBSERVATION

2.3.4 EMERGING SATELLITE CONSTELLATIONS

2.4 COMPUTER VISION FOR SATELLITE APPLICATIONS

2.4.1 CLASSICAL FEATURE DETECTION METHODS

2.4.2 EARTH FEATURE TRACKING AND LANDMARK RECOGNITION

2.5 VISION-BASED POSE ESTIMATION TECHNIQUES

2.5.1 CAMERA-BASED NAVIGATION SYSTEMS

2.5.2 GEOMETRIC POSE ESTIMATION METHODS

2.6 STATE ESTIMATION AND SENSOR FUSION

2.6.1 FILTERING TECHNIQUES FOR SATELLITE APPLICATIONS

2.6.2 MULTI-SENSOR FUSION ARCHITECTURES

2.6.3 ROBUSTNESS AND RELIABILITY TECHNIQUES

2.7 EARTH-TRACKING SYSTEMS FOR SATELLITE POSE ESTIMATION

MODELLING

3.1 INTRODUCTION

This project focuses on the pose estimation of a satellite using satellite images. This is essentially a localisation problem and requires a realistic description of the system. The aim of this chapter is to sufficiently define the problem and the proposed solution. Estimation algorithms are discussed and an estimator is chosen to solve the localisation problem. Further, attitude representations of a rigid body are introduced along with the dynamic and kinematic models used to describe a satellite in inertial space. Attention is given to quaternion attitude representations along with their propagation using angular rates.

3.2 PROBLEM DEFINITION

A satellite orbiting Earth in the Earth-Centered Inertial (ECI) reference frame performs Earth observation missions, continuously capturing high-resolution imagery of the planet's surface for scientific, commercial, or operational purposes. To fulfill mission objectives effectively, the satellite must provide not only high-quality imagery but also precise geographic information about observed areas. This requires accurate knowledge of the satellite's six-degree-of-freedom pose (three-dimensional position and three-dimensional attitude) relative to the ECI frame at the moment each image is captured.

Traditional satellite pose determination relies on external systems such as Global Navigation Satellite Systems (GNSS) and ground-based tracking networks. However, this thesis investigates an autonomous approach where the satellite performs "visual navigation" by identifying known ground features in its imagery and using these observations to determine its orbital state. The satellite essentially performs "reverse GPS" - instead of receiving position signals from space, it observes recognizable landmarks on Earth's surface and computes its pose from these visual references.

The core technical challenge lies in the transformation from raw imagery to precise pose estimates. This involves several interdependent problems: **(1) Feature Detection** - identifying which pixels in the imagery correspond to cataloged landmarks among millions of pixel observations; **(2) Geometric Inversion** - solving the complex inverse problem of determining six-dimensional pose from two-dimensional image projections of three-dimensional landmarks with known geographic coordinates; and **(3) Uncertainty Management** - handling measurement noise, feature detection errors, and dynamic orbital motion in real-time. This thesis assumes the availability of a pre-established catalog of ground features with precisely known geographic coordinates in the ECI frame. The feature matching problem - associating detected image features with specific catalog entries - is considered solved through prior knowledge of the observed terrain and existing geographic databases.

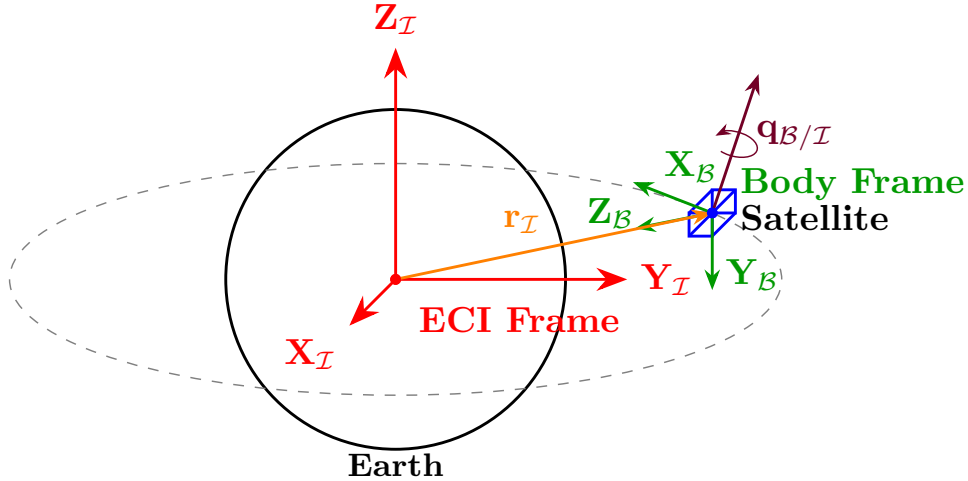


Figure 3.1: Satellite pose estimation concept showing orbital geometry, reference frames

This problem structure aligns with a simplified version of the Simultaneous Localization and Mapping (SLAM) framework. In this context, **localization** corresponds to determining the satellite's pose relative to the ECI frame using observations of cataloged features, while the **mapping** component is reduced to feature catalog utilization rather than creation. Since the geographic locations of observable features are assumed known a priori, the primary focus becomes the pose estimation problem given established feature correspondences.

The satellite's pose estimation system must account for the dynamic nature of orbital motion, the geometric relationship between the camera frame and satellite body frame, and the projection characteristics of the imaging system, while maintaining computational efficiency suitable for real-time onboard processing.

3.3 REFERENCE FRAME TRANSFORMATIONS

In this masters we are going to encounter a few different reference frames. To accurately create the measurement model we should have an understanding of all the different reference models and how to transform from one to another

3.3.1 LATITUDE, LONGITUDE AND ALTITUDE

The latitude, longitude of a feature or the position of the satellite is denoted with the \mathcal{L} . The latitude of a feature is the position of how high or low it is above the equator, having a range of -90° to 90° . The longitude is based on the Greenwich meridian, a longitude line that passes through the north- and south pole, it has a range of -180° to 180° . The altitude is measured from the "WGS84" elliptical globe.

$$\mathbf{r}_{\mathcal{L}} = \begin{bmatrix} \lambda \\ \phi \\ h \end{bmatrix} \quad (3.1)$$

3.3.2 EARTH CENTERED EARTH FIXED

The Earth Centered Earth Fixed reference frame is represented by the \mathcal{F} and is very similar to the \mathcal{L} reference frame with the z-axis aligned with the north pole and the x-axis points at the crossing of the Prime Meridian and the Equator, where the y-axis completes the right hand rule. The x, y and z-axis is defined in kilometers. To convert from \mathcal{L} to \mathcal{F} is to use a "WGS84" transform. Where WGS84 stands for World Geodetic System 1984, which is the standard coordinate system used for Global Positioning System (GPS). The WGS84 transformation uses a reference ellipsoid that uses a semi-major axis of 6,378 km and a flattening of $1/298.2$.

$$\mathbf{A}_{\mathcal{L}}^{\mathcal{F}} = f(\text{WGS84}) \quad (3.2)$$

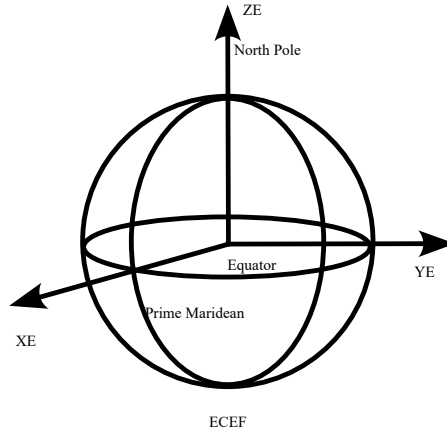


Figure 3.2: This figure represents the Earth Centered Earth Fixed reference frame with the X-axis defined in the direction of the equator and primemaridean with z-axis defined as the north pole and the y-axis completing the right had rule.

3.3.3 EARTH CENETERD INERTIAL

The Earth Centered Inertial reference fream (ECI) refrenced by \mathcal{I} shares a reference frame axis with the ECEF, but is rotated about the z-axis. This rotation is governed by the rotation speed of the earth ω_e which is 7.2921×10^{-5} rad/s and time t . To transform from the ECEF reference frame to the ECI reference frame one should rotate the Earth clockwise e.i.

$$\mathbf{A}_{\mathcal{F}}^{\mathcal{I}} = R(\omega_e t) = \begin{bmatrix} \cos(-\omega_e t) & -\sin(-\omega_e t) & 0 \\ \sin(-\omega_e t) & \cos(-\omega_e t) & 0 \\ 0 & 0 & 1 \end{bmatrix} \quad (3.3)$$

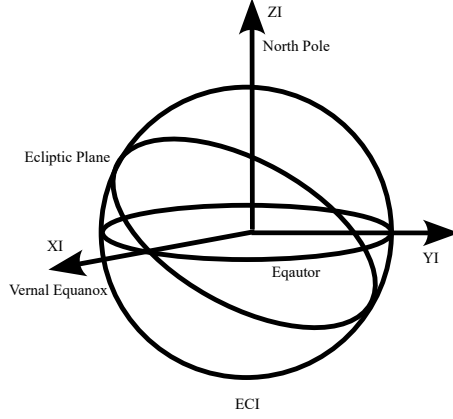


Figure 3.3: This figure represents the Earth Centered Inertial Reference frame with the x-axis defined in the direction of the vernal equinox, which is defined as the crossing of the ecliptic plane and the equator, the z-axis is defined as the north pole and the y-axis completes the right hand rule.

3.3.4 ORBITAL REFERENCE FRAME

The orbital reference frame used is the Local Vertical Local Horizon (LVLH) denoted by \mathcal{O} . **The LVLH frame is a rotating, orbit-attached coordinate system commonly used in spacecraft dynamics. It moves with the satellite and is defined relative to its orbit around Earth.** The x-axis is the "Local Horizon" also called "along track" pointing forward it is tangent to the orbit and points in the direction of motion. The z-axis is the local vertical and is also called the Nadir direction, it points to the barycenter of the system, in this case the center of the Earth. The y-axis is called the cross track it completes the right handed system. It points out of the orbital plane, typically the angular momentum vector direction (normal to the orbit plane).

if \mathbf{r} is the position vector of the satellite and \mathbf{v} is the velocity vector of the satellite. The equation for the reference frame is:

$$\bar{z}_{\mathcal{O}} = -\frac{\mathbf{r}}{\|\mathbf{r}\|} \quad (3.4)$$

$$\bar{y}_{\mathcal{O}} = \frac{\mathbf{r} \times \mathbf{v}}{\|\mathbf{r} \times \mathbf{v}\|} \quad (3.5)$$

$$\bar{x}_{\mathcal{O}} = \bar{y}_{\mathcal{O}} \times \bar{z}_{\mathcal{O}} \quad (3.6)$$

For this reference frame there should also be a reference frame translation introduced. Which is done by subtracting \mathbf{r} from the vector

$$\mathbf{f}_{\mathcal{O}} = \mathbf{A}_{\mathcal{I}}^{\mathcal{O}} \times (\mathbf{f}_{\mathcal{I}} - \mathbf{r}_{\mathcal{I}}) \quad (3.7)$$

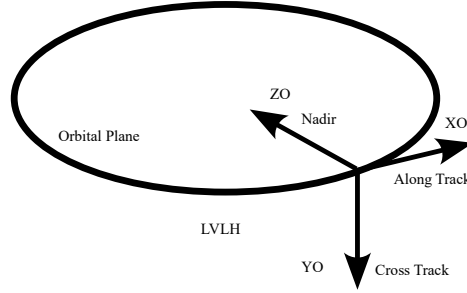


Figure 3.4: This figure represent the Local Vertical Local Horizon Reference frame, more commonly referred to as the orbital reference frame. In the orbital reference frame the z-axis is defined as Nadir, meaning that it always points to the center of mass perfectly parallel to the orbital plane, the x-axis is defined as the vector tangential to the plane, also known as the along track vector, and y is the completion of the right hand rule.

3.3.5 BODY REFERENCE FRAME

The body reference frame denoted by \mathcal{B} is the reference frame of the satellite body itself, with the center point referenced as the center of mass of the satellite body. with the z-axis defined as the yaw, x-axis defined as the roll and the y-axis defined as the pitch of the satellite. With the body frame z-axis and the orbital reference frame as aligned at initialisation

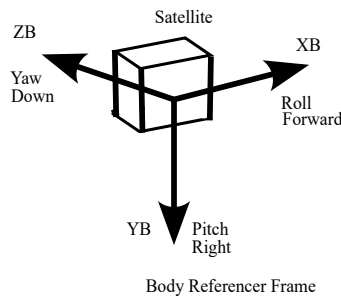


Figure 3.5

3.3.6 CAMERA REFERENCE FRAME

The camera reference frame denoted by \mathcal{C} . In many Earth Observation missions the camera has its own reference frame defined relative to the Earth. Where the x-axis is pointing directly to the Earth's surface indicating the camera's roll axis, with the y-axis representing the pitch axis represents an angle ahead or behind of the orbit and the z-axis representing the yaw axis.

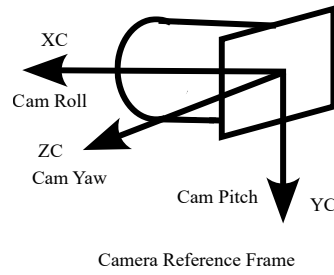


Figure 3.6

$$\mathbf{f}_C = \mathbf{A}_O^C \times \mathbf{f}_O \quad (3.8)$$

3.3.7 IMAGE REFERENCE FRAME

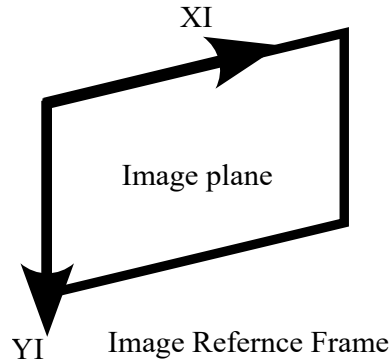


Figure 3.7

3.3.8 EAST - NORTH - UP

3.4 RIGID BODY MECHANICS

3.4.1 KINEMATICS

The pose of a rigid body in a reference frame consists of the position and attitude of the body. The attitude, or orientation of a body-fixed reference frame to a known reference frame. This is usually represented by a rotation matrix, often referred to as a direction cosine Matrix (DCM). A rotation about a single coordinate axis is referred to as a coordinate rotation. A coordinate rotation about the x-,y- and z-axes with angles ϕ , θ and ψ , of the body can be respectively describes as, [Willem de Jong p.23]

$$R_x(\phi) = \begin{bmatrix} 1 & 0 & 0 \\ 0 & \cos(\phi) & \sin(\phi) \\ 0 & -\sin(\phi) & \cos(\phi) \end{bmatrix} \quad (3.9)$$

$$R_y(\theta) = \begin{bmatrix} \cos(\phi) & 0 & -\sin(\phi) \\ 0 & 1 & 0 \\ \sin(\phi) & 0 & \cos(\phi) \end{bmatrix} \quad (3.10)$$

$$R_z(\psi) = \begin{bmatrix} \cos(\phi) & \sin(\phi) & 0 \\ -\sin(\phi) & \cos(\phi) & 0 \\ 0 & 0 & 1 \end{bmatrix} \quad (3.11)$$

Any rotation in 3D space can be described by three coordinate rotations. The DCM describing the attitude of the target in the camera reference frame (CRF), \mathbf{A}_C^B , can be represented by three Euler angles. Each of the angles corresponds to one coordinate rotation. The order of the Euler 1-2-3 rotation, shown in Figure 3.5, is expressed as

$$\mathbf{A}_C^B = R_x(\phi)R_y(\theta)R_z(\psi) \quad (3.12)$$

$$\begin{bmatrix} a_{1,1} & a_{1,2} & a_{1,3} \\ a_{2,1} & a_{2,2} & a_{2,3} \\ a_{3,1} & a_{3,2} & a_{3,3} \end{bmatrix} \quad (3.13)$$

$$\begin{bmatrix} C\theta C\psi & C\theta S\psi & -S\theta \\ S\phi S\theta C\psi - C\phi S\psi & S\phi S\theta S\psi + C\phi C\psi & S\phi C\theta \\ C\phi S\theta C\psi + S\phi S\psi & C\phi S\theta S\psi - S\phi C\psi & C\phi C\theta \end{bmatrix} \quad (3.14)$$

Where S is the sine function and C is the cosine function. The Euler angles are calculated as follows

$$\phi = \arctan 2 \left(\frac{a_{2,3}}{a_{3,3}} \right) \quad (3.15)$$

$$\theta = \arctan 2 \left(\frac{-a_{1,3}}{\sqrt{a_{1,1}^2} + \sqrt{a_{1,2}^2}} \right) \quad (3.16)$$

$$\psi = \arctan 2 \left(\frac{a_{1,2}}{a_{1,1}} \right) \quad (3.17)$$

mathematical singularities occur when using Euler angles to represent large rotations. When both $a_{1,1}$ and $a_{1,2}$ in Equation ?? are zero, the expressions for ψ and θ are undefined. This is known as *gimbal lock*, where the changes in the first and third Euler angles are indistinguishable when the second angle nears a critical value. Alternatively, the DCM can be described using quaternions, which do not have these singularities. The quaternion rotation in Figure ?? is expressed by the Euler axis $\bar{\mathbf{e}} = [e_x, e_y, e_z]^T$ and the angle θ

$$\mathbf{q} = \begin{bmatrix} q_s \\ q_x \\ q_y \\ q_z \end{bmatrix} = \begin{bmatrix} \cos(\theta/2) \\ e_x \sin(\theta/2) \\ e_y \sin(\theta/2) \\ e_z \sin(\theta/2) \end{bmatrix} \quad (3.18)$$

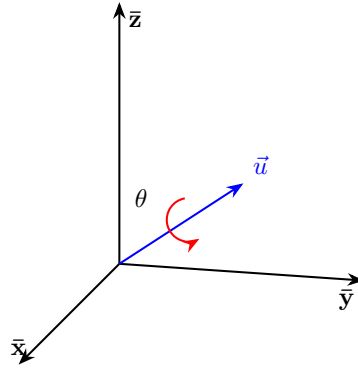


Figure 3.8: Quaternion Rotation

The DCM as a function of Quaternion set is expressed as,

$$\mathbf{A}_C^B = \begin{bmatrix} q_s^2 + q_x^2 - q_y^2 - q_z^2 & 2(q_x q_y - q_s q_z) & 2(q_x q_z + q_s q_y) \\ 2(q_x q_y + q_s q_z) & q_s^2 - q_x^2 + q_y^2 - q_z^2 & 2(q_y q_z - q_s q_x) \\ 2(q_x q_z - q_s q_y) & 2(q_y q_z + q_s q_x) & q_s^2 - q_x^2 - q_y^2 + q_z^2 \end{bmatrix} \quad (3.19)$$

Using the normalisation constraint, $q_s^2 + q_x^2 + q_y^2 + q_z^2 = 1$, the DCM Simplifies to,

$$\mathbf{A}_C^B = \begin{bmatrix} 1 - 2(q_y^2 + q_z^2) & 2(q_x q_y - q_s q_z) & 2(q_x q_z + q_s q_y) \\ 2(q_x q_y + q_s q_z) & 1 - 2(q_x^2 + q_z^2) & 2(q_y q_z - q_s q_x) \\ 2(q_x q_z - q_s q_y) & 2(q_y q_z + q_s q_x) & 1 - 2(q_x^2 + q_y^2) \end{bmatrix} \quad (3.20)$$

The body-fixed angular rates of the satellite in CRF, ω_C^B , is expressed as a function of quaternions by,

$$\omega_C^B = \begin{bmatrix} \omega_{bx} \\ \omega_{by} \\ \omega_{bz} \end{bmatrix} = 2 \begin{bmatrix} -q_x & q_s & -q_z & q_y \\ -q_3 & q_4 & q_1 & -q_2 \\ -q_4 & -q_3 & q_2 & q_s \end{bmatrix} \begin{bmatrix} \dot{q}_s \\ \dot{q}_x \\ \dot{q}_y \\ \dot{q}_z \end{bmatrix} \quad (3.21)$$

Inversly the quaternion rates as a function of the body rates are,

$$\begin{bmatrix} \dot{q}_s \\ \dot{q}_x \\ \dot{q}_y \\ \dot{q}_z \end{bmatrix} = \frac{1}{2} \begin{bmatrix} 0 & -\omega_{bx} & -\omega_{by} & -\omega_{bz} \\ \omega_{bx} & 0 & \omega_{bz} & -\omega_{by} \\ \omega_{by} & -\omega_{bz} & 0 & \omega_{bx} \\ \omega_{bz} & \omega_{by} & -\omega_{bx} & 0 \end{bmatrix} \begin{bmatrix} q_s \\ q_x \\ q_y \\ q_z \end{bmatrix} \quad (3.22)$$

Quaternions will be used throughout this thesis for attitude representations. Quaternions do not have ambiguity regarding the order of rotations and the rotation is around a well-defined axis. The sin and cosine elements of the rotation matrix are already encoded in the quaternion form of the DCM. Therefore, only one matrix operation is required for attitude transforms, where Euler angles require three.

3.4.2 DYNAMICS

3.4.2.1 TRANSLATIONAL DYNAMICS

For the translational dynamics, Newton's second law governs the linear motion of the satellite with mass m . The discrete-time position and velocity propagation equations are:

$$\mathbf{r}_t = \mathbf{r}_{t-1} + \mathbf{v}_t \Delta t + \frac{1}{2m} \mathbf{F}(t) \Delta t^2 \quad (3.23)$$

$$\mathbf{v}_t = \mathbf{v}_{t-1} + \frac{1}{m} \mathbf{F}(t) \Delta t \quad (3.24)$$

where $\mathbf{F}(t)$ represents the net external force acting on the satellite. For the orbital environment considered in this work, where external perturbations are negligible compared to gravitational forces, and given that precise mass properties may not be available, the translational motion can be approximated using kinematic models where the current velocity depends primarily on the previous velocity state.

In orbital mechanics the \mathbf{F} is proportional to the distance \mathbf{r} of the center of mass where the gravitational force is governed by the following equation.

$$\ddot{\mathbf{r}} = \mathbf{F}\mathbf{u}_r \quad (3.25)$$

$$\ddot{\mathbf{r}} = \frac{-\mu}{\|\mathbf{r}\|^3} \mathbf{u}_r \quad (3.26)$$

The acceleration of the space craft can be influenced by different factors like \mathbf{F}_G gravity, \mathbf{F}_{J_2} J2 perturbations, \mathbf{F}_{drag} atmospheric drag, \mathbf{F}_{sol} solar radiation pressure and other perturbations \mathbf{F}_{misc} .

This will mean the total force on the satellite would become

$$\mathbf{F}_{total} = \mathbf{F}_G + \mathbf{F}_{J_2} + \mathbf{F}_{drag} + \mathbf{F}_{sol} + \mathbf{F}_{misc} \quad (3.27)$$

But as we are only going to model LEO (Low Earth Orbits) for a short period of time only the \mathbf{F}_G and \mathbf{F}_{J_2} is considered.

Modelling the J2 perturbation is modelled in ECI using the following equation

$$\mathbf{a}_{J_2} = \frac{3}{2} * J_2 * \frac{\mu R_E}{\|\mathbf{r}\|^5} \begin{bmatrix} r_x(1 - 5\frac{z^2}{r^2}) \\ r_y(1 - 5\frac{z^2}{r^2}) \\ r_z(3 - 5\frac{z^2}{r^2}) \end{bmatrix} \quad (3.28)$$

Where

- * μ is Earth's gravitational parameter.
- * R_E is the radius of the Earth.
- * J_2 is the J2 factor
- * \mathbf{r} is the satellite position in ECI

3.4.2.2 ROTATIONAL DYNAMICS

The rotational dynamics of a rigid body satellite can be described using the Newton-Euler equations, which are applicable to all rigid inertial bodies. The angular momentum of the satellite is expressed as:

$$\dot{\mathbf{H}} = \frac{d\mathbf{H}}{dt} = \mathbf{I}\dot{\boldsymbol{\omega}} \quad (3.29)$$

where \mathbf{H} represents the angular momentum vector and \mathbf{I} is the diagonalized moment of inertia tensor about the satellite's principal axes. In the absence of external torques, the

rotational kinematics of a rigid satellite about its center of mass can be described by Euler's rotational equations:

$$I_{xx}\dot{\omega}_x = \omega_y\omega_z(I_{yy} - I_{zz}) \quad (3.30)$$

$$I_{yy}\dot{\omega}_y = \omega_x\omega_z(I_{zz} - I_{xx}) \quad (3.31)$$

$$I_{zz}\dot{\omega}_z = \omega_x\omega_y(I_{xx} - I_{yy}) \quad (3.32)$$

where I_{xx} , I_{yy} , and I_{zz} are the principal moments of inertia, which remain constant and depend on the satellite's mass distribution and geometric configuration.

The stability characteristics of the satellite's rotational motion are governed by its mass distribution. According to Marsden and Ratiu, rotation about the major and minor principal axes is inherently stable, while rotation about the intermediate axis exhibits unstable behavior. Under constant energy conditions, any initial rotation about the intermediate axis will gradually redistribute energy to the major and minor axes through nutation effects.

To propagate the quaternion representing the satellite's attitude over time, the quaternion derivative must first be computed. The time derivative of the quaternion $\mathbf{q}_{B/I}$, which describes the rotation from the inertial frame to the body frame, is calculated using quaternion multiplication with the angular velocity vector:

$$\dot{\mathbf{q}}_{B/I} = \frac{1}{2}(\mathbf{q}_{B/I} \otimes \boldsymbol{\omega}) \quad (3.33)$$

where $\boldsymbol{\omega} = [\omega_x, \omega_y, \omega_z]^T$ is the angular velocity vector expressed in the body frame. Expanding this quaternion multiplication yields:

$$\dot{\mathbf{q}}_{B/I} = \frac{1}{2} \begin{bmatrix} q_{B/I,0}\omega_x - q_{B/I,3}\omega_y + q_{B/I,2}\omega_z \\ q_{B/I,3}\omega_x + q_{B/I,0}\omega_y - q_{B/I,1}\omega_z \\ -q_{B/I,2}\omega_x + q_{B/I,1}\omega_y + q_{B/I,0}\omega_z \\ -q_{B/I,1}\omega_x - q_{B/I,2}\omega_y - q_{B/I,3}\omega_z \end{bmatrix} \quad (3.34)$$

where $q_{B/I,0}$, $q_{B/I,1}$, $q_{B/I,2}$, and $q_{B/I,3}$ are the scalar and vector components of the quaternion, respectively.

The quaternion integration is performed using a simple Euler integration scheme. First, the quaternion is propagated forward in time using:

$$\bar{\mathbf{q}}_{B/I}(t + \Delta t) = \mathbf{q}_{B/I}(t) + \dot{\mathbf{q}}_{B/I}\Delta t \quad (3.35)$$

where $\bar{\mathbf{q}}_{B/I}(t + \Delta t)$ represents the unnormalized quaternion after integration. Since quaternion integration may introduce numerical errors that violate the unit quaternion constraint, the result must be renormalized:

$$\mathbf{q}_{B/I}(t + \Delta t) = \frac{\bar{\mathbf{q}}_{B/I}(t + \Delta t)}{\|\bar{\mathbf{q}}_{B/I}(t + \Delta t)\|} \quad (3.36)$$

This normalization step ensures that the quaternion maintains its unit magnitude, preserving the validity of the attitude representation.

3.5 SENSOR MODELLING

3.5.1 GPS MEASUREMENT MODEL

In the simulation, GPS measurements are generated using the same underlying dynamics as the truth model, which is based on the two-body problem. This ensures consistency between the true satellite motion and the measurement framework. However, to emulate realistic sensor behavior, the GPS measurements are corrupted by both noise and drift.

The GPS measurement model is expressed as:

$$\mathbf{z}_{GPS}(t) = \mathbf{x}_{\text{true}}(t) + \boldsymbol{\eta}_{GPS}(t) + \mathbf{d}_{GPS}(t), \quad (3.37)$$

where:

- * $\mathbf{z}_{GPS}(t)$ is the observed GPS measurement at time t ,
- * $\mathbf{x}_{\text{true}}(t)$ is the true state of the system as propagated by the two-body equations of motion,
- * $\boldsymbol{\eta}_{GPS}(t)$ represents zero-mean Gaussian measurement noise, and
- * $\mathbf{d}_{GPS}(t)$ is the GPS drift.

The drift component models the slow, unbounded accumulation of error that is characteristic of certain classes of low-cost GPS receivers. It is implemented as a random walk process:

$$\mathbf{d}_{GPS}(t) = \mathbf{d}_{GPS}(t - \Delta t) + \mathbf{q}_{GPS}(t), \quad (3.38)$$

where:

- * $\mathbf{d}_{GPS}(t - \Delta t)$ is the drift at the previous timestep,
- * $\mathbf{q}_{GPS}(t)$ is a zero-mean stochastic increment modeling the drift rate, typically drawn from a Gaussian distribution:

$$\mathbf{q}_{GPS}(t) \sim \mathcal{N}(0, \sigma_d^2 \mathbf{I}). \quad (3.39)$$

This formulation captures both short-term measurement variability through $\boldsymbol{\eta}_{GPS}(t)$ and long-term bias trends via $\mathbf{d}_{GPS}(t)$, allowing for more realistic testing and evaluation of estimation algorithms under degraded or imperfect sensing conditions.

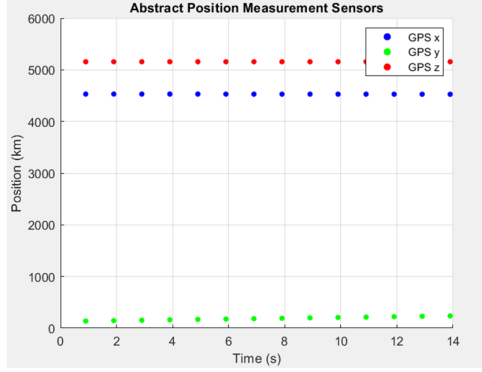


Figure 3.9

[Insert Image of Modelled GPS Results](#)

3.5.2 GYROSCOPE MEASUREMENT MODEL

The gyroscope provides a measurement of the angular velocity of the body frame relative to the inertial frame, expressed in the body frame. This quantity is denoted as $\boldsymbol{\omega}_{B/I}^B$, and forms a critical part of attitude determination and estimation systems.

To simulate a realistic sensor, the gyroscope measurement is corrupted by both random noise and a time-varying bias, or drift. The measurement model is given by:

$$\mathbf{z}_{\text{Gyro}}(t) = \boldsymbol{\omega}_{B/I}^B(t) + \boldsymbol{\eta}_{\text{Gyro}}(t) + \mathbf{d}_{\text{Gyro}}(t), \quad (3.40)$$

where:

- * $\mathbf{z}_{\text{Gyro}}(t)$ is the observed gyroscope measurement at time t ,
- * $\boldsymbol{\omega}_{B/I}^B(t)$ is the true angular velocity of the body frame relative to the inertial frame,
- * $\boldsymbol{\eta}_{\text{Gyro}}(t)$ is zero-mean Gaussian noise representing short-term measurement error, and
- * $\mathbf{d}_{\text{Gyro}}(t)$ is the gyroscope drift, modeled as a time-varying bias.

The drift is modeled as a random walk process, capturing slow variations in the sensor bias over time:

$$\mathbf{d}_{\text{Gyro}}(t) = \mathbf{d}_{\text{Gyro}}(t - \Delta t) + \mathbf{q}_{\text{Gyro}}(t), \quad (3.41)$$

with the stochastic increment defined as:

$$\mathbf{q}_{\text{Gyro}}(t) \sim \mathcal{N}(0, \sigma_g^2 \mathbf{I}), \quad (3.42)$$

where σ_g^2 represents the drift rate variance of the gyroscope.

This model allows for the representation of both high-frequency noise and long-term integration drift, which are commonly observed in practical inertial measurement units (IMUs). Incorporating this model into the estimation framework enables more robust and accurate state reconstruction in the presence of sensor imperfections.

3.5.3 STAR TRACKER

3.5.4 COARSE SUN SENSOR

The Coarse Sun Sensor (CSS) is a fundamental attitude sensing instrument in nanosatellite systems, providing an estimate of the Sun direction relative to the satellites body frame. This subsection outlines the modeling approach for simulating CSS measurements, including the transformation of reference frames, sensor configuration, noise characteristics, and estimation logic.

Sun Vector in Inertial Frame The Sun vector is modeled in the Earth-Centered Inertial (ECI) frame as a fixed unit vector pointing in the $+X$ direction:

$$\mathbf{S}_{\mathcal{I}} = \begin{bmatrix} 1 & 0 & 0 \end{bmatrix}^{\top} \quad (3.43)$$

This simplified model assumes that the Sun direction does not vary during the simulation.

Transformation to Body Frame To simulate the Sun vector in the satellite's body frame, the inertial vector is rotated using the satellite's true attitude quaternion. The corresponding direction cosine matrix (DCM) is derived as:

$$\mathbf{S}_{\mathcal{B}} = R_{\mathcal{I}}^{\mathcal{B}} \cdot \mathbf{S}_{\mathcal{I}} \quad (3.44)$$

where $R_{\mathcal{I}}^{\mathcal{B}}$ is the DCM from the inertial to body frame.

Sensor Layout and Response The CubeSat is equipped with six coarse sun sensors, one on each face, aligned along the $\pm X$, $\pm Y$, and $\pm Z$ body axes (see Figure ??). Each sensor has a cosine response:

$$z_i = \max \left(0, \hat{\mathbf{n}}_i^{\top} \mathbf{S}_{\mathcal{B}} \right), \quad i = 1, \dots, 6 \quad (3.45)$$

where $\hat{\mathbf{n}}_i$ is the normal vector of the i -th sensor surface.

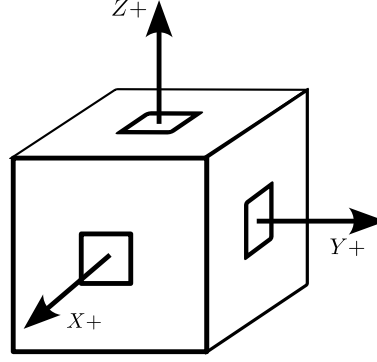


Figure 3.10: Orientation of the six coarse sun sensors on the CubeSat

Measurement Noise Each CSS reading is perturbed with zero-mean Gaussian noise. The noise standard deviation σ is specified in degrees and converted to radians:

$$\mathbf{z}_{\text{CSS}} = \max(0, \mathbf{z}_{\text{CSS}} + \mathcal{N}(0, \sigma^2)), \quad \sigma = \text{deg} \rightarrow \text{rad}(\text{CSS}_{\text{noise}}) \quad (3.46)$$

Negative readings are clamped to zero since physical sensors cannot detect negative intensity.

Sun Vector Estimation The estimated Sun vector in the body frame is reconstructed using a weighted sum of the face normals:

$$\hat{\mathbf{S}}_B = \sum_{i=1}^6 z_i \cdot \hat{\mathbf{n}}_i \quad (3.47)$$

The result is normalized to produce a unit vector:

$$\hat{\mathbf{S}}_B = \frac{\hat{\mathbf{S}}_B}{|\hat{\mathbf{S}}_B|} \quad (3.48)$$

[Add some results](#)

3.5.5 MAGNETOMETER

The magnetometer measurement is modeled as a unit vector pointing along the direction of the Earth's magnetic field as observed from the satellite body frame. To approximate this field, a simplified model is used in which the magnetic field points toward the geographic North Pole and is tangential to the Earth's surface at the satellite's location, with an optional dip angle to simulate inclination.

Step 1: Earth-Fixed Transformation

To determine the orientation of the magnetic field relative to the Earth-fixed frame, the satellite position vector $\mathbf{r}_{\mathcal{I}}$ in the inertial (ECI) frame is first transformed to the Earth-fixed (ECEF) frame using a rotation matrix that accounts for Earth's rotation angle at time t :

$$\mathbf{r}_{\mathcal{R}} = R_{\mathcal{I}}^{\mathcal{R}}(t) \cdot \mathbf{r}_{\mathcal{I}} \quad (3.49)$$

where $R_{\mathcal{I}}^{\mathcal{R}}(t)$ is a time-dependent rotation matrix based on the Earth rotation rate ω_e .

Step 2: Direction to Magnetic North

The geographic North Pole is approximated by a fixed point on the Z-axis of the Earth-fixed frame:

$$\mathbf{p}_{NP,\mathcal{R}} = \begin{bmatrix} 0 \\ 0 \\ R_E \end{bmatrix} \quad (3.50)$$

The direction vector from the satellite to the North Pole is then computed as:

$$\mathbf{d}_{NP} = \mathbf{p}_{NP,\mathcal{R}} - \mathbf{r}_{\mathcal{R}} \quad (3.51)$$

Step 3: Tangential Magnetic Field Model

The local radial unit vector from the Earth's center is:

$$\mathbf{u}_{r,\mathcal{R}} = \frac{\mathbf{r}_{\mathcal{R}}}{|\mathbf{r}_{\mathcal{R}}|} \quad (3.52)$$

To simulate a magnetic field that is tangential to Earth's surface, the component of \mathbf{d}_{NP} in the radial direction is removed:

$$\mathbf{z}_{\text{Mag},\mathcal{R}} = \mathbf{d}_{NP} - (\mathbf{d}_{NP} \cdot \mathbf{u}_{r,\mathcal{R}})\mathbf{u}_{r,\mathcal{R}} \quad (3.53)$$

This tangential field vector is then normalized:

$$\mathbf{z}_{\text{Mag},\mathcal{R}} = \frac{\mathbf{z}_{\text{Mag},\mathcal{R}}}{|\mathbf{z}_{\text{Mag},\mathcal{R}}|} \quad (3.54)$$

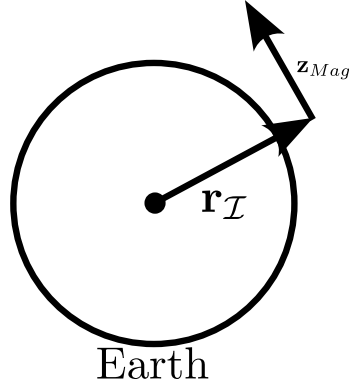


Figure 3.11

Step 4: Dip Angle Adjustment

To simulate magnetic inclination, a rotation about the local East direction is applied to tilt the magnetic field by a dip angle δ , which is measured downward from the local horizontal plane:

$$\mathbf{z}_{Mag,\mathcal{R}}^{\text{incl}} = \cos(\delta) \mathbf{z}_{Mag,\mathcal{R}} + \sin(\delta) (\mathbf{e}_{\text{East}} \times \mathbf{z}_{Mag,\mathcal{R}}) \quad (3.55)$$

Here, \mathbf{e}_{East} is the local east direction, obtained via:

$$\mathbf{e}_{\text{East}} = \frac{\mathbf{u}_{r,\mathcal{R}} \times \mathbf{z}_{Mag,\mathcal{R}}}{|\mathbf{u}_{r,\mathcal{R}} \times \mathbf{z}_{Mag,\mathcal{R}}|} \quad (3.56)$$

Step 5: Reference Frame Transformations

The inclined magnetic field vector is transformed back to the inertial frame using:

$$\mathbf{z}_{Mag,\mathcal{I}} = R_{\mathcal{R}}^{\mathcal{I}}(t) \cdot \mathbf{z}_{Mag,\mathcal{R}}^{\text{incl}} \quad (3.57)$$

The final transformation to the spacecraft body frame is performed using the spacecraft attitude quaternion $\mathbf{q}_{\mathcal{B}}^{\mathcal{I}}$, resulting in:

$$\mathbf{z}_{Mag,\mathcal{B}} = R(\mathbf{q}_{\mathcal{B}}^{\mathcal{I}}) \cdot \mathbf{z}_{Mag,\mathcal{I}} \quad (3.58)$$

where $R(\mathbf{q})$ is the direction cosine matrix corresponding to the quaternion \mathbf{q} .

Step 6: Measurement Noise

To simulate realistic sensor output, a small-angle random rotation is applied to the vector $\mathbf{z}_{Mag,\mathcal{B}}$ to represent magnetometer noise. This is modeled by sampling a noise rotation axis and applying a perturbation angle drawn from a Gaussian distribution with a standard deviation σ_{noise} (in radians). The rotation is implemented via a noise quaternion and applied to the magnetic field vector.

Step 7: Output

The final estimated magnetometer vector $\hat{\mathbf{z}}_{\text{Mag},\mathcal{B}}$ is normalized and output for use in state estimation:

$$\hat{\mathbf{z}}_{\text{Mag},\mathcal{B}} = \frac{\mathbf{z}_{\text{Mag},\mathcal{B}}}{|\mathbf{z}_{\text{Mag},\mathcal{B}}|} \quad (3.59)$$

This provides a realistic simulation of a three-axis magnetometer, with both geographic dependence and sensor-level noise, for use in spacecraft attitude determination or estimation filters.

3.5.6 TRIAD ATTITUDE ESTIMATION

The TRIAD (Tri-Axial Attitude Determination) algorithm is a deterministic method used to estimate a spacecraft's attitude from two independent, non-collinear direction measurements expressed in both the body and inertial frames. In this work, the TRIAD method is applied using sun vector measurements from a coarse sun sensor and magnetic field measurements from a three-axis magnetometer.

Step 1: Sensor Measurements in Body Frame

Let $\mathbf{s}_{\mathcal{B}}$ denote the unit vector pointing toward the Sun in the body frame, and $\mathbf{m}_{\mathcal{B}}$ the unit magnetic field vector in the body frame. These vectors are obtained from sensor measurements and normalized:

$$\mathbf{s}_{\mathcal{B}} = \frac{\mathbf{s}_{\mathcal{B}}}{|\mathbf{s}_{\mathcal{B}}|}, \quad \mathbf{m}_{\mathcal{B}} = \frac{\mathbf{m}_{\mathcal{B}}}{|\mathbf{m}_{\mathcal{B}}|} \quad (3.60)$$

Step 2: Reference Vectors in Inertial Frame

The inertial-frame counterparts to the measured vectors are defined as follows:

- The Sun vector in the inertial (ECI) frame is approximated by the unit vector:

$$\mathbf{s}_{\mathcal{I}} = \begin{bmatrix} 1 \\ 0 \\ 0 \end{bmatrix} \quad (3.61)$$

- The magnetic field vector in the inertial frame, $\mathbf{m}_{\mathcal{I}}$, is computed based on the spacecraft position $\mathbf{r}_{\mathcal{I}}$, a user-defined magnetic dip angle, and Earth's rotation:

$$\mathbf{m}_{\mathcal{I}} = \text{MagnetometerModel}(\mathbf{r}_{\mathcal{I}}, t, \omega_e, \delta) \quad (3.62)$$

Both reference vectors are normalized:

$$\mathbf{s}_{\mathcal{I}} = \frac{\mathbf{s}_{\mathcal{I}}}{|\mathbf{s}_{\mathcal{I}}|}, \quad \mathbf{m}_{\mathcal{I}} = \frac{\mathbf{m}_{\mathcal{I}}}{|\mathbf{m}_{\mathcal{I}}|} \quad (3.63)$$

Step 3: Constructing Orthogonal Triads

Two orthonormal vector triads are constructed from the body and reference measurements.

- In the inertial frame:

$$\mathbf{v}_1^{\mathcal{I}} = \mathbf{s}_{\mathcal{I}} \quad (3.64)$$

$$\mathbf{v}_2^{\mathcal{I}} = \frac{\mathbf{s}_{\mathcal{I}} \times \mathbf{m}_{\mathcal{I}}}{|\mathbf{s}_{\mathcal{I}} \times \mathbf{m}_{\mathcal{I}}|} \quad (3.65)$$

$$\mathbf{v}_3^{\mathcal{I}} = \mathbf{v}_1^{\mathcal{I}} \times \mathbf{v}_2^{\mathcal{I}} \quad (3.66)$$

- In the body frame:

$$\mathbf{v}_1^{\mathcal{B}} = \mathbf{s}_{\mathcal{B}} \quad (3.67)$$

$$\mathbf{v}_2^{\mathcal{B}} = \frac{\mathbf{s}_{\mathcal{B}} \times \mathbf{m}_{\mathcal{B}}}{|\mathbf{s}_{\mathcal{B}} \times \mathbf{m}_{\mathcal{B}}|} \quad (3.68)$$

$$\mathbf{v}_3^{\mathcal{B}} = \mathbf{v}_1^{\mathcal{B}} \times \mathbf{v}_2^{\mathcal{B}} \quad (3.69)$$

These vectors form right-handed orthonormal bases (triads) in their respective frames.

Step 4: Attitude Rotation Matrix

The attitude rotation matrix $R_{\mathcal{I}}^{\mathcal{B}}$, which rotates vectors from the inertial frame to the body frame, is computed by aligning the inertial and body triads:

$$T_{\mathcal{I}} = [\mathbf{v}_1^{\mathcal{I}} \quad \mathbf{v}_2^{\mathcal{I}} \quad \mathbf{v}_3^{\mathcal{I}}], \quad T_{\mathcal{B}} = [\mathbf{v}_1^{\mathcal{B}} \quad \mathbf{v}_2^{\mathcal{B}} \quad \mathbf{v}_3^{\mathcal{B}}] \quad (3.70)$$

$$R_{\mathcal{I}}^{\mathcal{B}} = T_{\mathcal{B}} \cdot T_{\mathcal{I}}^{\top} \quad (3.71)$$

Step 5: Quaternion Conversion

The attitude quaternion $\mathbf{q}_{\mathcal{B}}^{\mathcal{I}}$ corresponding to the rotation matrix $R_{\mathcal{I}}^{\mathcal{B}}$ is computed using a standard matrix-to-quaternion conversion:

$$\mathbf{q}_{\mathcal{B}}^{\mathcal{I}} = \text{rotm2quat}(R_{\mathcal{I}}^{\mathcal{B}}) \quad (3.72)$$

This quaternion is expressed in scalar-first format:

$$\mathbf{q}_{\mathcal{B}}^{\mathcal{I}} = [q_s \quad q_x \quad q_y \quad q_z]^{\top} \quad (3.73)$$

The TRIAD method thus yields a closed-form attitude estimate without optimization or iteration. While it is highly efficient, its accuracy depends on the orthogonality and noise properties of the sensor measurements.

3.6. CONCLUSION

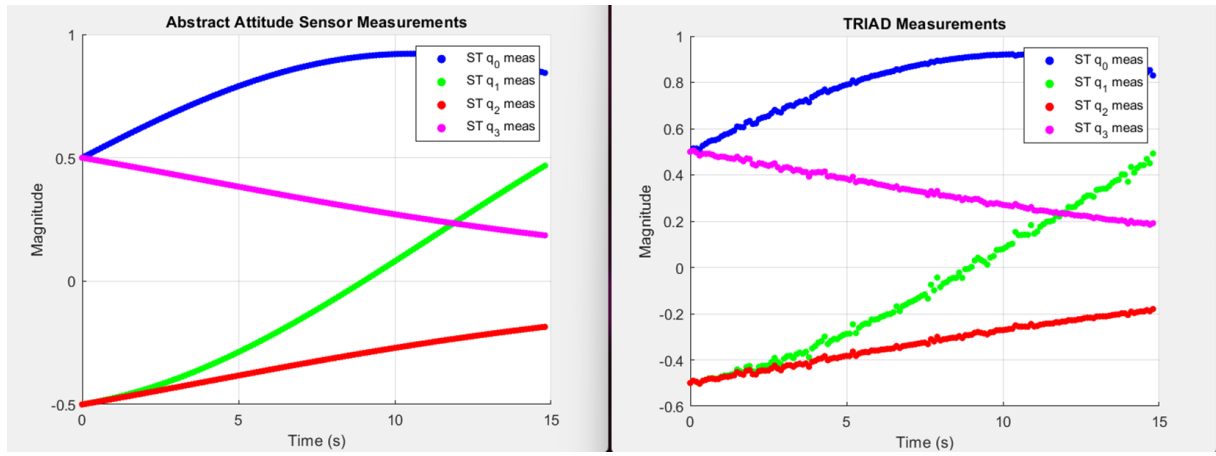


Figure 3.12

3.6 CONCLUSION

IMAGE PROCESSING

4.1 INTRODUCTION

4.2 PINHOLE CAMERA MODEL

The ideal pinhole camera can be described as a plane and an optical center (a.k.a) the pinhole. Light will travel from an object throught the optical center. And hit the plane at the opposite end of the optical center. The distance between the optical center and the plane is called the focal length f .

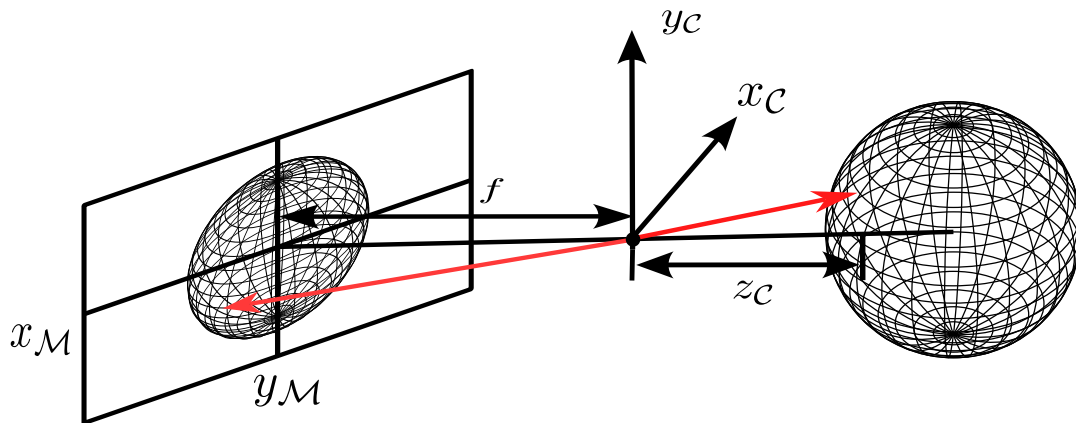


Figure 4.1: PinHole Model

The equation for the pinhole camera model is the following.

$$\begin{bmatrix} x_{\mathcal{M}} \\ y_{\mathcal{M}} \\ 1 \end{bmatrix} = \frac{-f}{z_c} \begin{bmatrix} x_c \\ y_c \\ z_c \end{bmatrix} \quad (4.1)$$

As we can see in the figure this also causes the image to flip.

Also images are measured with the x-axis going from right to left and the y-axis going from top to bottom so one more transformation needs to be done.

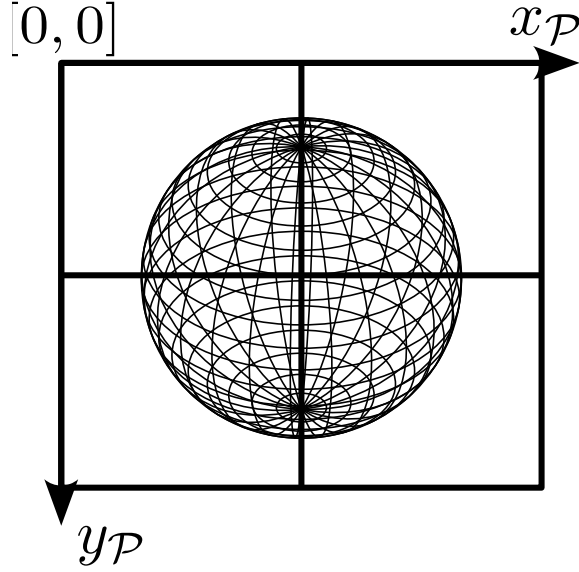


Figure 4.2: Image Plane

$$\begin{bmatrix} x_{\mathcal{P}} \\ y_{\mathcal{P}} \end{bmatrix} = \begin{bmatrix} -x_{\mathcal{M}} + \frac{\text{ImgWidth}}{2} \\ y_{\mathcal{M}} + \frac{\text{ImgHeight}}{2} \end{bmatrix} \quad (4.2)$$

4.2.1 INTRINSIC CAMERA PARAMETERS

4.2.2 EXTRENSIC CAMERA PARAMETERS

4.3 SATELLITE IMAGE CHARACTERISTICS

4.3.1 GROUND SAMPLE DISTANCE

4.3.2 IMAGING GEOMETRY

4.4 FEATURE DETECTION AND DESCRIPTION

4.4.1 CLASSICAL FEATURE DETECTORS

4.4.2 FEATURE DESCRIPTION

4.5 MEASUREMENT EXTRACTION

4.5.1 FEATURE-TO-MEASUREMENT TRANSFORMATION

4.5.2 EARTH TRACKER ALGORITHM

4.5.3 GEOLOCATION PROCESS

STATE ESTIMATION

5.1 INTRODUCTION

5.2 EXTENDED KALMAN FILTER

This section describes the element of of recursive estimators

5.3 SYSTEM MODELLING

5.3.1 MOTION MODEL

5.3.2 MEASUREMENT MODEL

5.4 SIMULATION

5.5 PRACTICAL CONSIDERATION

5.5.1 NUMBER OF FEATURES

5.5.2 OUTLIERS

5.6 CONCLUSION

SYSTEM INTEGRATION

6.1 SYSTEM DIAGRAM

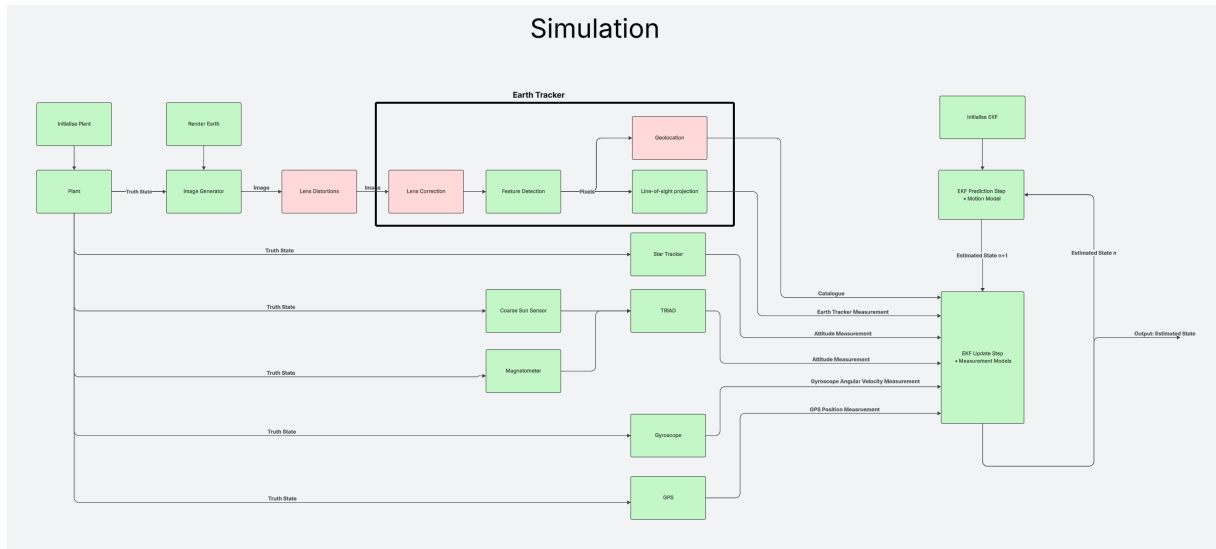


Figure 6.1: Image Plane

6.2 SYSTEM INITIALIZATION

The orbital system is initialized using the following parameters:

- * **Latitude:** Initial geodetic latitude of the satellite.
- * **Longitude:** Initial geodetic longitude of the satellite.
- * **Altitude:** Initial altitude above the WGS84 ellipsoid.

- * **Roll (X-axis)**: Initial roll angle of the satellite body with respect to the orbital reference frame.
- * **Pitch (Y-axis)**: Initial pitch angle of the satellite body with respect to the orbital reference frame.
- * **Yaw (Z-axis)**: Initial yaw angle of the satellite body with respect to the orbital reference frame.

The geodetic latitude, longitude, and altitude are first converted to an inertial position vector using the WGS84 Earth model. This involves a transformation from the local geodetic frame to the Earth-Centered Earth-Fixed (ECEF) frame, followed by a rotation into the inertial frame:

$$\mathbf{r}_{\mathcal{I}} = T_{\mathcal{R}}^{\mathcal{I}} \left(T_{\mathcal{L}}^{\mathcal{R}}(\mathbf{r}_{\mathcal{L}}, \omega_e, t) \right) \quad (6.1)$$

To compute the initial velocity vector, it is assumed that the satellite is in a near-circular orbit, and thus its velocity vector is orthogonal to its position vector. While multiple solutions satisfy this constraint, the velocity direction is resolved using the local east unit vector, which is always tangential to the satellite's position on the Earth's surface. The eastward direction is given by:

$$\mathbf{u}_{\text{east}} = \frac{1}{\|\cdot\|} \begin{bmatrix} -\sin(\lambda) \\ \cos(\lambda) \\ 0 \end{bmatrix} \quad (6.2)$$

where λ is the geodetic longitude. The vector is normalized to obtain a unit direction. The magnitude of the orbital velocity is computed using the vis-viva equation:

$$\|\mathbf{v}\| = \sqrt{\frac{\mu}{\|\mathbf{r}\|}} \quad (6.3)$$

where μ is the standard gravitational parameter, and $\|\mathbf{r}\|$ is the norm of the inertial position vector.

The inertial velocity vector is then calculated as:

$$\mathbf{v}_{\mathcal{I}} = \|\mathbf{v}\| \cdot \mathbf{u}_{\text{east}} \quad (6.4)$$

[Add some pictures for visualisation](#)

The satellite's initial attitude is defined by two sequential quaternion rotations:

- * $q_{\mathcal{O}/\mathcal{I}}$: the quaternion representing the rotation from the inertial (ECI) frame \mathcal{I} to the orbital reference frame \mathcal{O} ,

* $q_{\mathcal{B}/\mathcal{O}}$: the quaternion representing the rotation from the orbital frame \mathcal{O} to the satellite body frame \mathcal{B} ,

These quaternions are constructed using the initial orbital position (from latitude, longitude, and altitude) and the initial roll, pitch, and yaw of the satellite body with respect to the orbital frame.

The total attitude of the satellite body with respect to the inertial frame is given by the quaternion composition:

$$q_{\mathcal{B}/\mathcal{I}} = q_{\mathcal{B}/\mathcal{O}} \otimes q_{\mathcal{O}/\mathcal{I}} \quad (6.5)$$

where \otimes denotes quaternion multiplication, performed right-to-left (i.e., the rotation $q_{\mathcal{O}/\mathcal{I}}$ is applied first, followed by $q_{\mathcal{B}/\mathcal{O}}$).

Reference Frame Alignment at Initialization At the simulation start time $t = 0$, it is assumed that the Earth-Centered, Earth-Fixed (ECEF) frame \mathcal{R} is aligned with the inertial frame \mathcal{I} . This is a common simplification used in orbital mechanics when time is initialized at a known Greenwich Mean Sidereal Time (GMST), typically zero. This alignment implies:

$$R_{\mathcal{R}}^{\mathcal{I}}(t = 0) = \mathbf{I}_{3 \times 3} \quad (6.6)$$

where $R_{\mathcal{R}}^{\mathcal{I}}$ is the rotation matrix from ECEF to ECI. This simplifies the initial attitude calculations and ensures consistent initialization across reference frames.

Angular Velocity Initialization The initial angular velocity of the satellite body is specified relative to the orbital frame:

$$\boldsymbol{\omega}_{\mathcal{B}/\mathcal{O}}^{\mathcal{B}} = \begin{bmatrix} \omega_x \\ \omega_y \\ \omega_z \end{bmatrix} \quad (6.7)$$

Since the ECI and ECEF frames are aligned at $t = 0$, and the orbital frame is defined in the ECI frame, this implies that the angular velocity of the body with respect to the inertial frame is initially equivalent to the angular velocity with respect to the orbital frame:

$$\boldsymbol{\omega}_{\mathcal{B}/\mathcal{I}}^{\mathcal{B}}(t = 0) = \boldsymbol{\omega}_{\mathcal{B}/\mathcal{O}}^{\mathcal{B}}(t = 0) \quad (6.8)$$

This relationship holds only at the initialization instant. As time progresses, the orbital frame rotates relative to the inertial frame due to the satellite's motion, and the

distinction between $\boldsymbol{\omega}_{\mathcal{B}/\mathcal{I}}$ and $\boldsymbol{\omega}_{\mathcal{B}/\mathcal{O}}$ becomes significant and must be handled accordingly in the attitude propagation.

EXPERIMENTS

7.1 INTRODUCTION

7.2 CONCLUSION

CONCLUSION AND FUTURE WORK

8.1 CONCLUSION

8.2 FUTURE WORK

REFERENCES

APPENDIX A

APPENDIX TITLE GOES HERE
